Chapter 5:

Sandalwood-derived Carbon Quantum Dots as Bioimaging Tools to Investigate the Toxicological Effects of Malachite Green in Model Organisms

5.1 Introduction

5.1.1 Threats Caused by Malachite Green in the Body

Malachite green (MG) is a cationic blue-green dye known to be used for years in paper, leather, silk, wool, cotton, jute and acrylic industries.[1,2] The diamino triarylmethane emerald dye crystals also finds applications as an efficient bioicide, laboratory staining agent and medical disinfectant that has been, historically, used in profusion as an effective parasiticide in aquaculture.[1,2,3] This practice came into question after Poe and Wilson (1983) found its residue in frozen fillets of channel catfish.[4,5] MG metabolically transforms into its leuco derivative, leucomalachite green (LMG), via interchangeable redox process after absorption in animal tissues and gets accumulated in various organs and viscera for a long time, many months in edible fish.[3] Although LMG does not pose clastogenic threats,[6] it still has harmful effects like long half-life and may oxidise back into MG.[4,7,8] MG can cause genotoxic and carcinogenic changes by introducing free DNA breaks, chromosomal aberrations and free radical generation.[3,9] It can cause severe damage, including tumours, in the hepatic, renal, thyroid, pulmonary system and the gonads which can affect the next generation progeny also.[1,3,4,10]

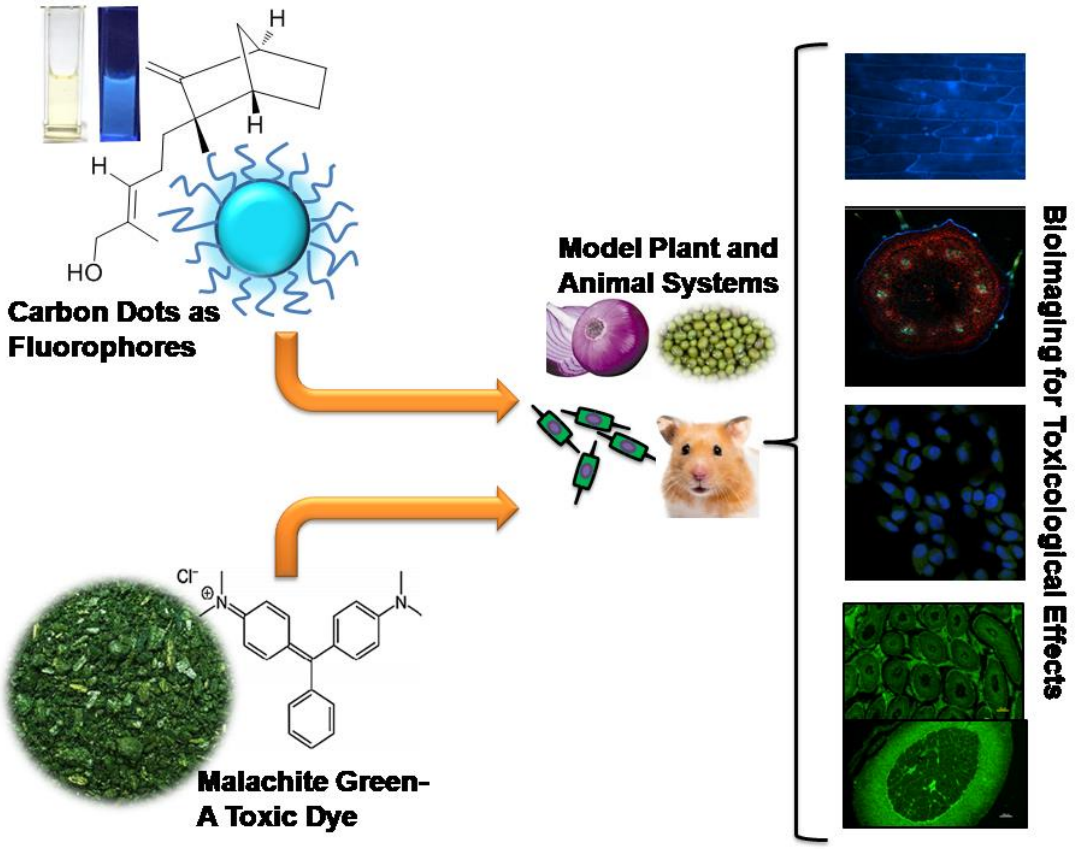

Figure 5.1: Schematic Illustrating the Bioimaging Studies Conducted on various plant (*Allium cepa, Vigna radiata*) and animal model systems (MG-63 osteoblast cell line, golden hamster) for investigating the toxicological effects of malachite green using sandalwood-derived carbon quantum dots as fluorescence probes

5.1.2 Unscrupulous Use of Malachite Green

In light of these findings, several countries banned the use of MG in consumables and aquaculture industry including USFDA, Canada and European Union. Still, the unscrupulous use of this dye is prevalent in many places due to its ease of synthesis, low cost and commercial availability.[1] Occupational exposure to workers in printing and textile industries is dangerous exposing them to chronic metabolic hazards.[9] Even after imposing government ban, vendors unscrupulously use MG in juices, sweets and even green vegetables for providing better customer appeal through brighter appearance.[9,11] A study showed how various high

temperature modes of cooking do not guarantee complete degradation of MG and LMG residue in food.[12] In some states of South India, it is easily available in green cow dung powder in local grocery shops even after being legally banned. This powder is generally believed to be safe owing to its natural green colour.[13] Green colour powder used in the festival of Holi, has been found to contain different concentrations of MG ranging from 0.3% to 85%. Shockingly, this colour can enter the eye and cause ocular damage threatening vision.[14] Surveillance studies have found the use of MG as a non-permitted food colouring agent not approved by US Food and Drug Administration.[4,15] It has been classified under category CIII by the joint FAO/WHO Expert Committee on Food Additives.[16] It has also been banned by US Environmental Protection Agency for use on any aquatic species.[16] Nonetheless, spurious use of MG is prevalent in many corners of the world.[15]

Proper investigation and understanding of the toxicological role of MG will not only have an impact on the environment but also help people to make conscious and informed decisions regarding their daily habits and lifestyle. The ionisation constant (pK) of MG is 6.9. On getting ionised in water they are greener at pH 4 (100% ionised), more blue as the pH gets increases (50% at pH 6.9) and finally forms leucoform precipitates at high pH (0% at pH 10.1).[3,17] The toxicity of MG is directly proportional to its exposure time, ions like Ca^{2+}, concentration and temperature.[3] It has been reported that intestinal microflora are capable of converting MG into LMG.[18] LMG seems to be highly lipid-soluble lending to its entry inside cells and nucleus. Alternative parasiticides, like humic acid, chlorine dioxide and Pyceze should be explored to replace MG.[3] Many recent attempts to detect MG have been made including advanced SERS microfluidic sensor with an LOD of 1-2 ppb and even simple calorimetric devices for domestic use with an LOD of 18 nM MG.[11,19]

5.1.3 The ill-effects of MG exposure on general biota

Damage caused by a particular chemical entity is difficult to understand in its entirety since chronic exposure slowly shows cumulative toxicological effects like cancer in any species after some time making it difficult to estimate the damage instantly.[9] The degree and locus of damage also varies from one species to the other. Data relating to the cytotoxicity, pathological damage and carcinogenicity of MG is archaic, obscure and limited employing outdated microscopy techniques.[16] As such it becomes very important to conduct detailed studies on finding the toxicological potential of MG using both *in vivo* and *in vitro* experimental model systems.

Unknown exposure to the dye also affects nearby flora and fauna. Free discharge of MG in water is a concern as it enters the aquatic food chain and may rebound in the form of edible fishes. It has been observed how water acts as a transport channel for such toxic chemicals that end up in the environment into the soil which is an important sink for materials.[20] Plants face the direct impact of such environmental contamination as these chemicals can penetrate cells easily. They are the cornerstones of most ecosystems and significantly contribute to the bioaccumulation of chemicals. The complexity surrounding the entry, interactions and pathological ill-effects of MG have often found contradictory conclusions leading to confusion in the minds of scientists. Research has been limited to understanding direct toxicity in mammalian models. Hence, it is crucial to throw some light into this topic in further detail.

5.1.4 Use of Sandalwood-derived CQDs for Bioimaging of the Adverse Effects of MG

Carbon Quantum Dots (CQDs) derived from natural sources have gained a lot of attention owing to their ease of synthesis, low cost, green one-pot synthesis method

without additional toxic reagents, excellent fluorescent properties, wavelength tunable emission, good photostability, biocompatibility and aqueous solubility.[21] They have been used for a wide range of applications like analyte sensing, optoelectronic device components, drug delivery and theranostics.[22] CQDs have proved to be amenable fluorescence markers and probes and have widely been employed for bioimaging.[23,24] They have several advantages over traditional fluorescent dyes like tuneable emission, biocompatibility, very low cost and facile synthesis. Sandalwood (*Santalum album*) has been used for centuries on account of their fragrant wood composed of primarily two isomers of santalol and is used for extracting its essential oils, ameliorating skin problems, for aromatherapy, cosmetics and for pharmaceuticals.[25] Since its composition is rich in sesquiterpenic alcohols like α-santalol, β-santalol, α-bisabalol, nuciferol, curcumen-12-ol, cis-lanceol, bergamatol and farnesol, the interplay and contribution of these functional groups was worth exploring converting sandalwood into CQDs.[26]

In this chapter, the application of CQDs as a fluorescent probe for better visualisation and understanding of changes in plant and animal tissue architecture and physiology because of exposure to MG has been studied. Sandalwood-derived CQDs have been synthesized using a green and eco-friendly approach via a facile one-step hydrothermal method. They possess excellent fluorescence properties with a quantum yield of 12% and average lifetime of 8.63 ns making them suitable tools for bioimaging. The toxicological effects of MG have been studied using model plant systems like onion bulb epidermal tissue and mung bean sprouts. Further, this study has been extended in animal cell lines and model i.e. *in vitro* and *in vivo* studies on MG-63 cell line and golden hamster models have also been carried out to understand the adverse effects of the dye.

5.2 Results and Discussions

To conduct a comprehensive study on the toxicological effects of malachite green, sandalwood-derived carbon quantum dots were synthesized. These CQDs were extensively characterized and were found to be very fluorescent making them ideal candidates for bioimaging. They were used as tools to understand the toxicology of malachite green in plant and animal models.

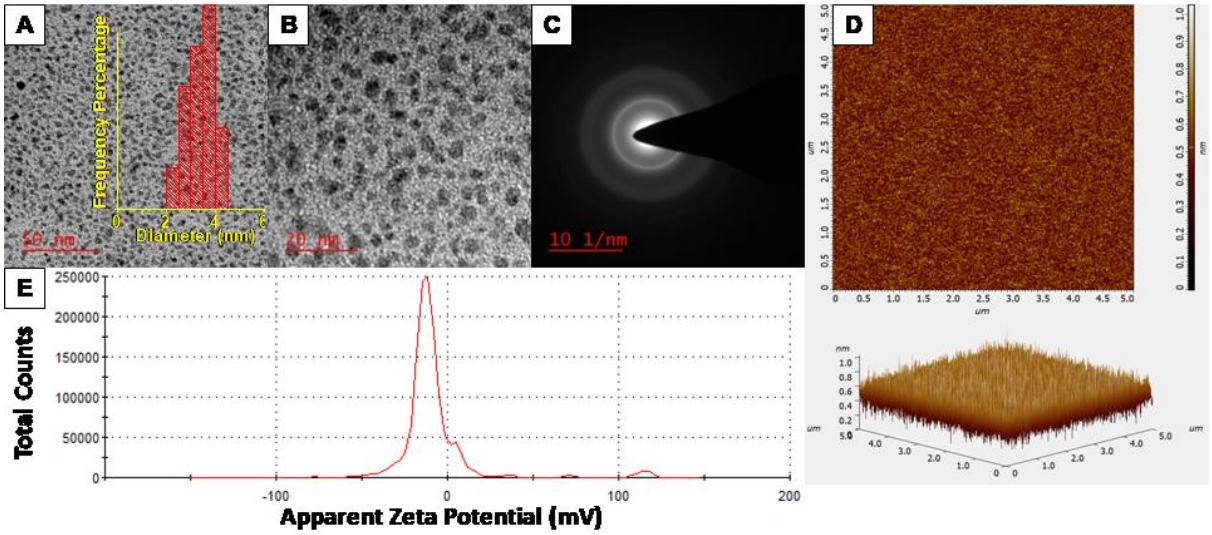

Figure 5.2: Morphological Characterisation of CQDs. (A-B) TEM showing Uniform Distribution of CQDs. (C) SAED Pattern of CQDs (D) AFM profile of CQDs (E) Zeta Potential of CQDs

5.2.1 Morphology and Surface Charge of the Sandalwood-derived CQDs

Transmission Electron Microscopy (TEM) was conducted to estimate the diameter and morphology of the CQDs. They were found to be monodispersed uniformly having a quasispherical shape (Figure 5.2A-B). Their diameter lay within the range of 2-4 nm averaging around 3.5 nm. This was also confirmed by the Atomic Force Microscopy (AFM) profile (Figure 5.2D). The Selected Area Electron Diffraction (SAED) pattern revealed the amorphous nature of the CQDs through

diffuse concentric rings (Figure 5.2C). Zeta potential measurement showed that the CQDs possessed a negative surface zeta potential of -13 mV (Figure 5.2E). This ensures the stability of the negatively charged CQDs on account of electrostatic repulsion between individual quantum dots as seen in most CQDs.

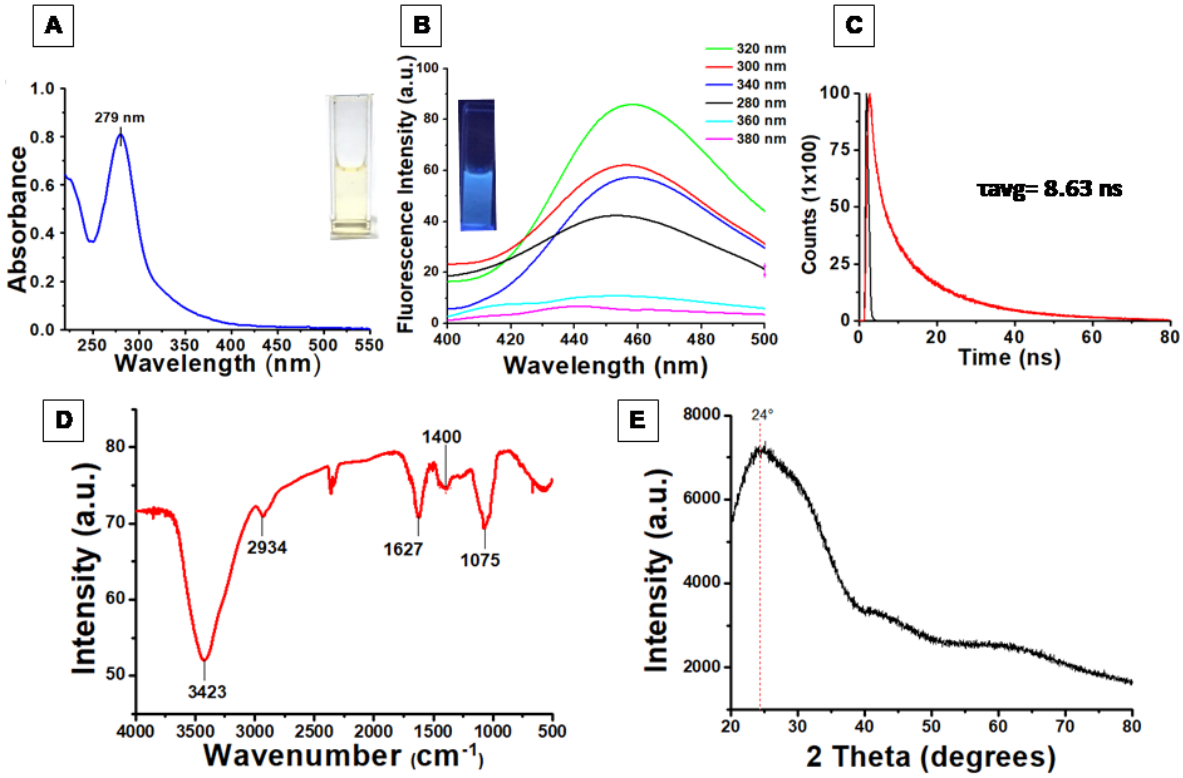

Figure 5.3: Optical and Structural Characterisation of CQDs. (A) UV-Vis Spectrum of CQDs (B) Photoluminescence Emission Spectra of CQDs excited at different wavelengths (C) Average lifetime of CQD Fluorescence (D) FTIR spectrum of CQDs (E) XRD profile of CQDs

5.2.2 Optical and Structural Properties of CQDs

The CQDs appeared light yellowish-brown in daylight and possessed fine aqueous solubility. The UV-Vis absorbance spectrum reveals maximum absorption in the UV-blue region (Figure 5.3A). A prominent peak at 279 nm is ascribed to n-π* electronic transitions from C=O functional groups as seen in earlier reports.[27-30] The most remarkable characteristic of CQDs is their intrinsic photoluminescence property.

An excitation-dependent fluorescence spectrum was observed with a Stokes' shift of 138 nm (Figure 5.2B). The excitation and emission wavelengths for maximum fluorescence intensity were found at 320 nm and 458 nm respectively. The quantum yield of the CQDs was found to be 12% using quinine sulphate as reference in 0.1 M H_2SO4.[29] Fluorescence lifetime of CQDs at room temperature was measured to be 8.63 ns by fitting into a tri-exponential function with an R^2 value of 0.9995 (Figure 5.2C). This observed lifetime is exceptionally higher than most average lifetimes of CQDs derived from natural sources having an average value usually less than 4 ns. This opens their potential for use in optoelectronic, bioimaging and sensing devices. Guo et al synthesized "biodots" having an average lifetime of 10.44 ns.[31] They proposed that sp^2 carbon–like centers from cytosine form luminescence centers or chromophores for the photoluminescence. Another group found citric acid and ethylenediamine derived CQDs having very high lifetimes of 7.9 and 13.2 ns. They concluded that closing non-radiative channels prolongs fluorescence lifetime.[32] Higher degree of conformational rigidity, oxidation state and polarity are also correlated with longer lifetime.[33] Multiexponential emission decay is often found in CQDs which may arise from rapid band gap transitions between different discrete states or may also indicate the fast radiative recombination of multiple exciton species contributed by carboxyl, hydroxyl and other oxygen species.[34]

To shed light into the surface functional group composition of the CQDs, Fourier Transform Infrared Spectroscopy (FTIR) was conducted. The spectrum revealed multiple functional groups (Figure 5.3D). A prominent peak at 3423 cm^{-1} indicates the presence of free and hydrogen bonded hydroxyl groups (OH) as well as amine stretch (NH) since the peak is relatively narrow. These groups may lend to the hydrophilicity of the CQDs. A small peak at 2931 cm^{-1} is indexed to alkyl stretch

(CH). A sharp peak at 1627 cm^{-1} is ascribed to either amine bending (NH) or amide/alkene stretch (C=O, C=C). A stubby peak at 1400 cm^{-1} may indicate hydroxyl bending (OH). Finally, the peak at 1075 cm^{-1} may be contributed by C-O/C-N stretch. The results confirm the presence of oxygen and nitrogen containing functional groups on the surface of CQDs improving their aqueous solubility. X-ray diffraction pattern (XRD) is in agreement with the SAED pattern and confirms that the graphitic surface of the CQDs was amorphous as indicated by a broad peak centred at 24° (Figure 5.3E). This may also indicate the presence of defects created by abundant functional groups which in turn make the hydrophilic CQDs stable for a long time without visible aggregation.

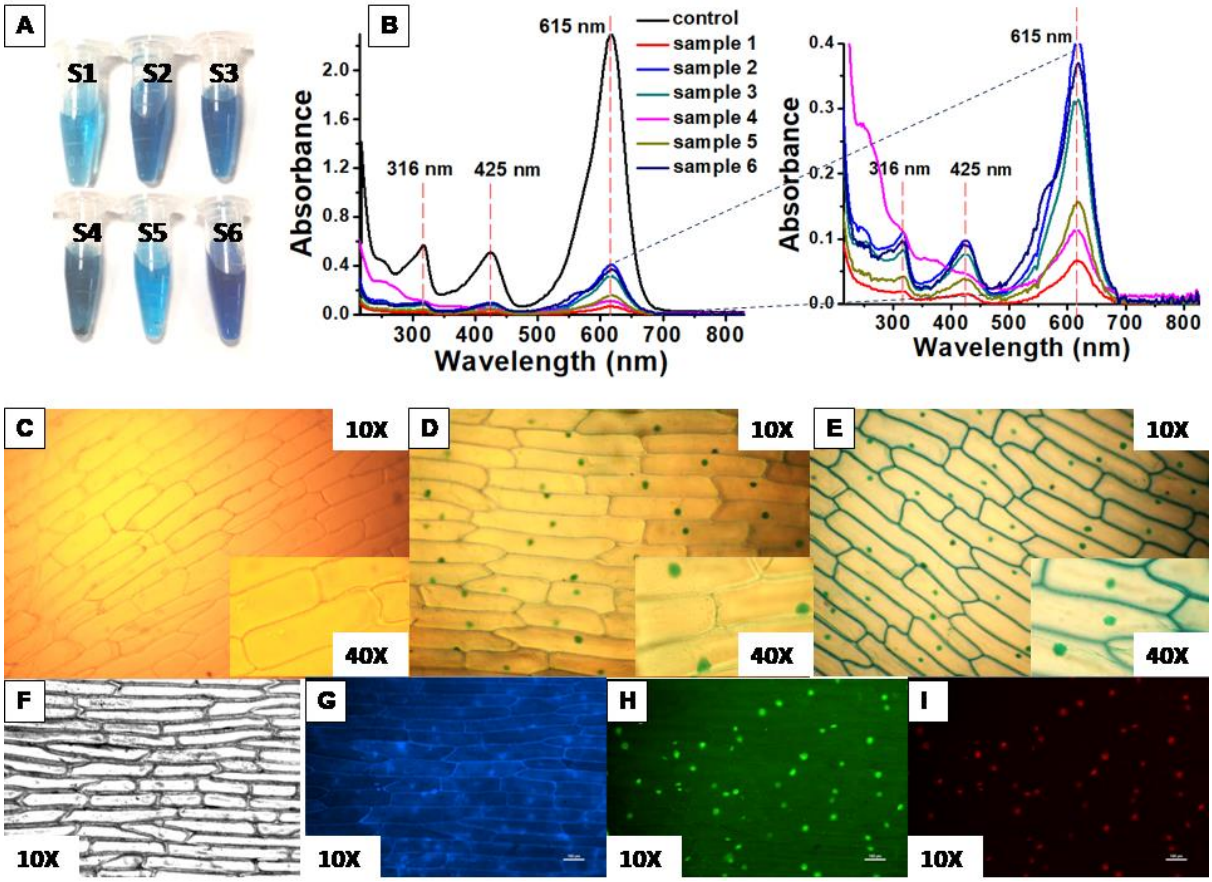

Figure 5.4: Testing Real Samples for the Presence of Malachite Green (A-B) Positive MG Spectra for All Tested Samples. Light microscopy images for onion bulb (*Allium cepa*) epidermal tissues for (C) control (0 mM MG) (D) 0.4 mM MG (E) 1 mM MG. Fluorescence microscopy images for 1 mM soaked onion bulb tissues using CQD as fluorescent stain (F-I)

5.2.3 Checking Local Green Colour Samples for the Presence of Malachite Green (MG)

To check the easy availability of MG in green colour samples, samples were procured from local shops. Out of the 6 green colour samples randomly obtained from local vendors, all the samples were positive for the signature absorbance profile of MG indicated by prominent peaks at 316 nm, 425 nm and 615 nm (Figure 5.4A-B). Following Beer-Lambert Law, Figure 5.4B clearly demonstrates that MG is present in all the samples in varying concentrations when compared to the control (27.4 µM).

The concentration for all samples and control to be measured was kept constant at 10 µg/ml for comparison. The rest of each sample might contain copper sulphate, additives and impurities to increase the bulk weight. Therefore, UV-Vis absorbance spectra can be easily used for routine scrutiny analysis of dyes like MG. This result shows how easily harmful dyes such as MG are commonly available in local shops also reflecting their demand for various uses during festivals and as general dyes. Ease of availability and very low price of dye packets attract few vendors to unscrupulously colour green vegetables to give them a fresher appealing look for the customers.[11] People may unknowingly ingest the dye during festivals like Holi when coloured water containing the dye enters eyes and mouth causing unprecedented damage.[14]

5.2.4 Dissection of MG Transport in Epidermal Onion (*Allium cepa*) Bulb Tissues

Rectangular cells of the epidermal layer of the onion bulb skin are very distinctly visible under an optical microscope owing to their large size (Figure 5.4C). This makes them ideal plant tissue models for observing changes caused by any toxic moiety. Since MG is a dye, its localisation is easily visible under a light microscope. After being soaked in 0.4 mM MG solution for 12 hours, the dye most noticeably localised in the nucleus of the plant cells showing their high affinity and passive migration towards DNA material (Figure 5.4D). This hints at how prone cells are towards any DNA damage that can be caused by the partially cationic dye which may strongly interact with the negatively charged DNA. As the concentration of the solution is increased to 1 mM, MG starts collecting within the cell wall of the plant cells (Figure 5.4E). This shows the affinity of MG for cellulosic fibres. Reports have hypothesized this adsorption affinity between MG-cellulosic fibres may be either due to electrostatic interactions or lipophilicity[1,35,36] or hydrophobic forces[14] leading to conformational changes in proteins. Lipophilic affinity of MG for membranes has also

been illustrated through the interaction between MG and lecithin liposomes.[37] Teichman reported MG affinity with phospholipids via interactions between amine groups in MG with basophilic groups in lipids.[17,38] The ultralow toxicity and feasibility in cell imaging make CQDs amenable bioimaging probes for plant tissues.[39,40] After immersing the 1 mM peel into CQD solution (0.33 mg/ml) for 6 hours and drying, it was viewed under fluorescence microscope to gain better structural changes caused by MG (Figure 5.4F-I). There were not any discernable histostructural changes in the onion tissues but CQDs seemed to co-localize within MG deposit-sites like the nuclei and cell walls as evidenced by bright fluorescence.[41] This hints at similarity in the affinity of MG and CQDs for cell structures and can be used in future to detect changes in cyto-architecture in growing saplings which is expected to yield more drastic toxicology-related changes as compared to adult plants which merely act as MG storage sites. Better resolution was observed for sample excited with UV filter (blue image) as compared to the red image. It is to be noted that the contact time with MG is proportional to the tissue concentration.[14] Another important point to consider is that the autofluorescence caused by the structural proteins and other biomolecules in the plant itself can cause interference with the fluorescence signal generated solely by the CQDs.[42]

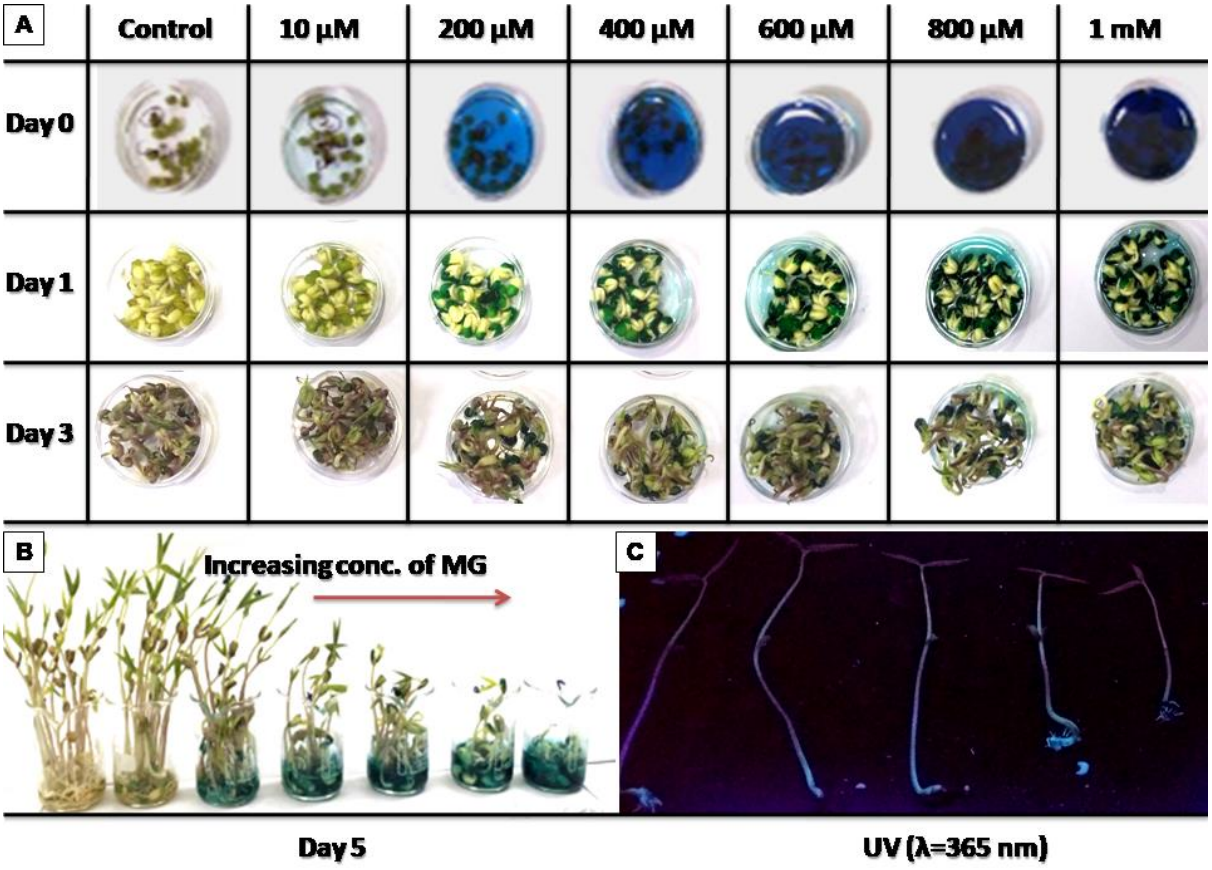

Figure 5.5: (A-B) Growth of mung beans (*Vigna radiata*) in the presence of different concentrations of MG (0-1 mM MG). (C) Fluorescence from CQDs under UV illumination at λ= 365 nm)

5.2.5 MG Toxicity Studies in Mung Beans (*Vigna Radiata*)

Phytotoxicity can be indicated by many physiological changes like reduced photosynthesis, poor germination rates and stunted growth of plants.[20] In order to study the physiological changes in plant growth on exposure to different concentrations of MG, mung plant (*Vigna radiata*) was selected as the model plant since it is rapid growing and easy to cultivate. It is a common indigenous crop and has been reported to be a bioindicator for metals like arsenic.[43] 6 different concentrations of MG in DI (10 µM, 200 µM, 400 µM, 600 µM, 800 µM and 1 mM) and control (no MG) were chosen as media for the plant seeds which were cultured for 5 days

hydroponically (Figure 5.5A-B). No additional growth promoters, nutrient supplements, or ions were added to avoid the complex interplay of all the media components. On day 0, the colour intensity of MG clearly reflected the increasing concentration of dye in solution. However, few hours later the colour of the dye visibly faded indicating rapid absorption by the dicot seeds. It has been previously reported how biomass has been used for efficient adsorption and even retrieval of MG.[44] Enzymes such as NADH-DCIP reductase and MG reductase have been found to play a role in decolourization of the dye in *S. cerevesiae*.[43] Day 1 seeds showed disjunction of the cotyledons after bursting and separation from the seed coat. The seed coats had adsorbed most of the dye as shown in figure. Internalization of MG does not indicate immediate toxic effects since plants have natural defence strategies like exclusion through cell wall or sequestration through vacuoles. Different regulator proteins like glutathione and phytochelatins may also play a role.[20] By day 3, a pair of leaves had started to appear forming the plumule. As the plants gained length by day 5, there was a remarkable difference in the lengths of the plants based on the dye concentration demonstrating potential toxicity contrary to the findings of Gopinathan et al. (Figure 5.5B).[45]

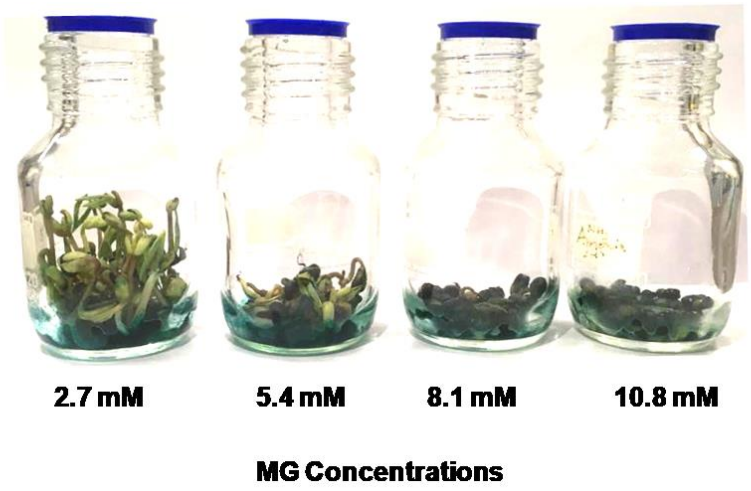

Figure 5.6: Growth experiment demonstrating LC_{LO}, the lowest lethal concentration at which seeds are unable to sprout and show no signs of germination

The LC_{LO} (Lowest Lethal Concentration) of MG has been described as the lowest concentration of MG at which no visible growth in seeds occurs and was found out to be 11 mM for *Vigna radiata* plants under ambient conditions (Figure 5.6). Relative root elongation (E) is a very important parameter to prove the phytotoxic effect of any chemical.[46] On day 6, one plant each from the sets were retrieved (0-0.8 mM MG) and washed several times with DI. Then they were placed in 0.33 mg/ml sandalwood CQD solution for 20 hours before viewing them under 365 nm UV illumination for tracking their fluorescence to see CQD uptake (Figure 5.5C). It is to be noted that the roots distinctly exhibit strong blue fluorescence since they are the first point of contact with the CQD solution and initiation site for their absorption. CQDs seem to stay longer in the MG-treated plants with stunted growth as compared to control plants which may have a developed a better transpiration and toxin elimination system than the MG-treated plants whose cellular responses seem to be affected. Fluorescence was not as coherent in the shoots, cotyledons or the leaves. This makes the roots better sites for fluorescence microscopy and imaging to avoid the autofluorescence from the plant itself.

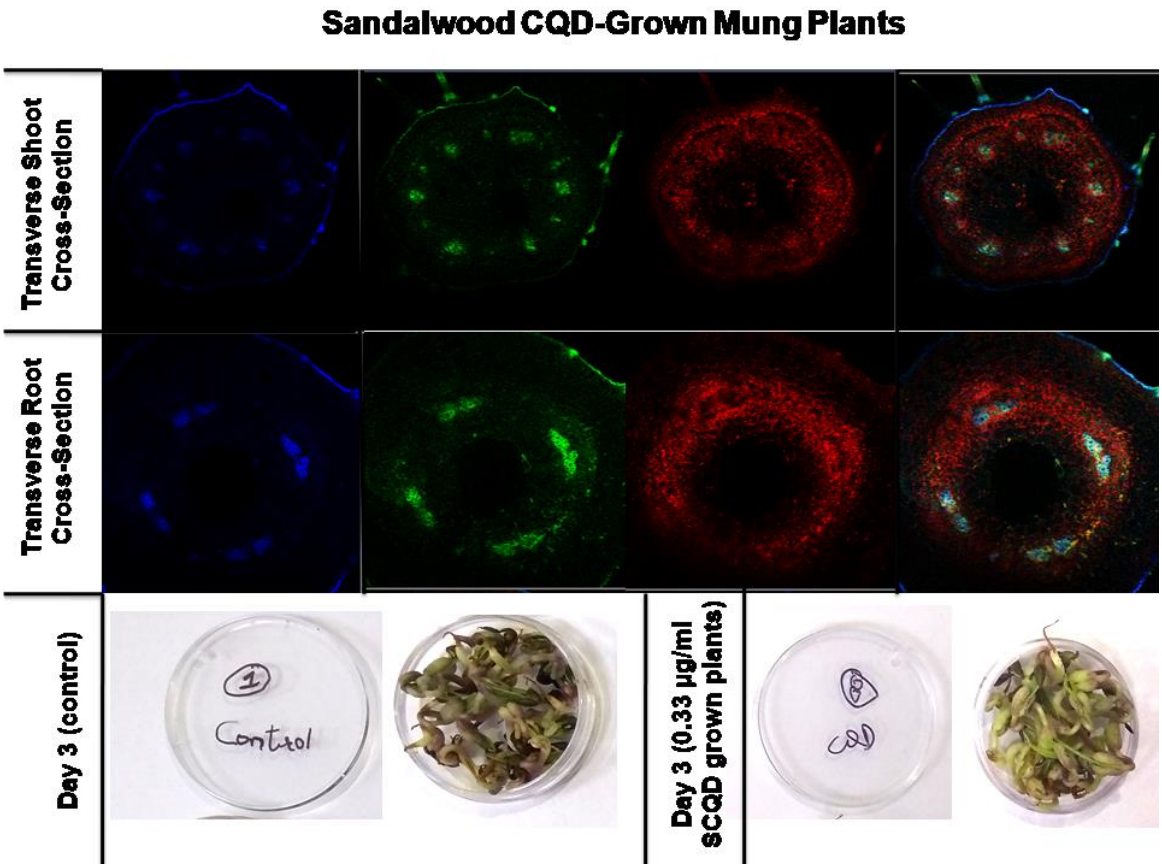

Figure 5.7: Mung bean (*Vigna radiata*) seeds grown in pure 100% sandalwood CQD solution (0.33 µg/ml) showing no effect on growth as compared to control plants

No significant difference in the growth of mung bean seeds was observed as compared to control when grown in pure sandalwood solution (0.33 mg/ml) (Figure 5.7). It has been reported that CQDs may enhance photosynthetic rate by promoting electron transfer, RUBISCO activity and chlorophyll content.[41,47] The good biocompatibility of the CQDs may be attributed to the natural source and green synthesis method.[41]

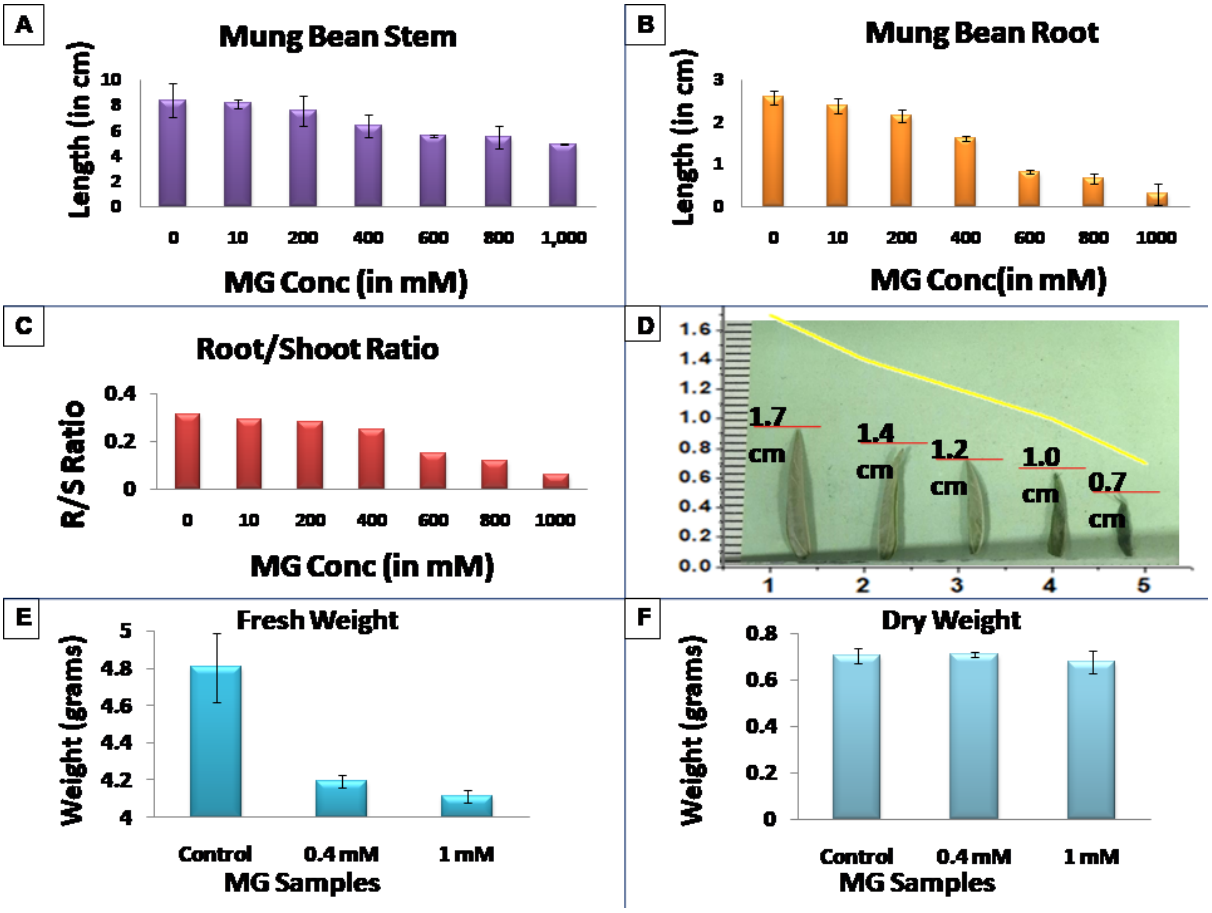

Figure 5.8: Physical Parameters Affected by Malachite Green (A) Shoot Length Affected by Increasing Concentration of MG (B) Root Length Affected by Increasing Concentration of MG (C) Root:Shoot Length Ratios for MG Treated Plants (0-1 mM MG) (D) Leaf Diameter Affected by Increasing Concentration of MG (E) Fresh Weight and (F) Dry Weight of Plants after Exposure to MG (0, 0.4, 1 mM MG)

5.2.6 Mung Plant Growth and Development Parameters for Assessing MG Toxicity

To observe the effects of MG toxicity on the plant growth, several parameters were selected for assessment after 6 days (Figure 5.8A-F). The length of the shoot and root were primarily checked for changes. Shoot length distinctively varied with increasing concentration of MG from an average value of 8.43 cm in control to 4.97 cm for 1 mM MG plant sample (Figure 5.8A). For root length the average value ranged from 2.6 cm for control seedling to 0.3 cm for 1 mM MG plant sample (Figure 5.8B). This clearly shows how MG is detrimental for the growth of plants as it retards

further mitotic activity by accumulation in the cells. As seen in the case of onion cells, the dye may easily penetrate the nucleus causing irreversible DNA damage causing the plant to cease further growth. The root/ shoot ratio was also estimated which showed a decreasing trend (Figure 5.8C). This could be possible because the root growth primarily gets retarded through intercellular signalling when exposed to a toxic compound. The longitudinal axis and surface area of the leaf was also reduced with increasing MG concentration reflecting growth retardation (Figure 5.8D). Marked difference of 1 cm was observed between control and 0.8 mM MG plant sample. Dry weight (DW) is another important parameter which helps in understanding the accumulation in biomass. No significant difference was seen in DW on increasing the dose of MG in the limited period of growth but fresh biomass weight decreased serially with increasing concentration (Figure 5.8E-F). This explains the higher water content in unaffected plants as compared to MG treated ones. Germination index (GI) and half life (T50) was not considered significant for this study since the plants showed 100% growth within very close time frames which could lead to erroneous conclusions. These studies demonstrate how deleterious effects caused by MG can affect non-target plants and organisms in soil ecosystems.[45,48] They may cause oxidative damage, cellular changes and lipid peroxidation.[43]

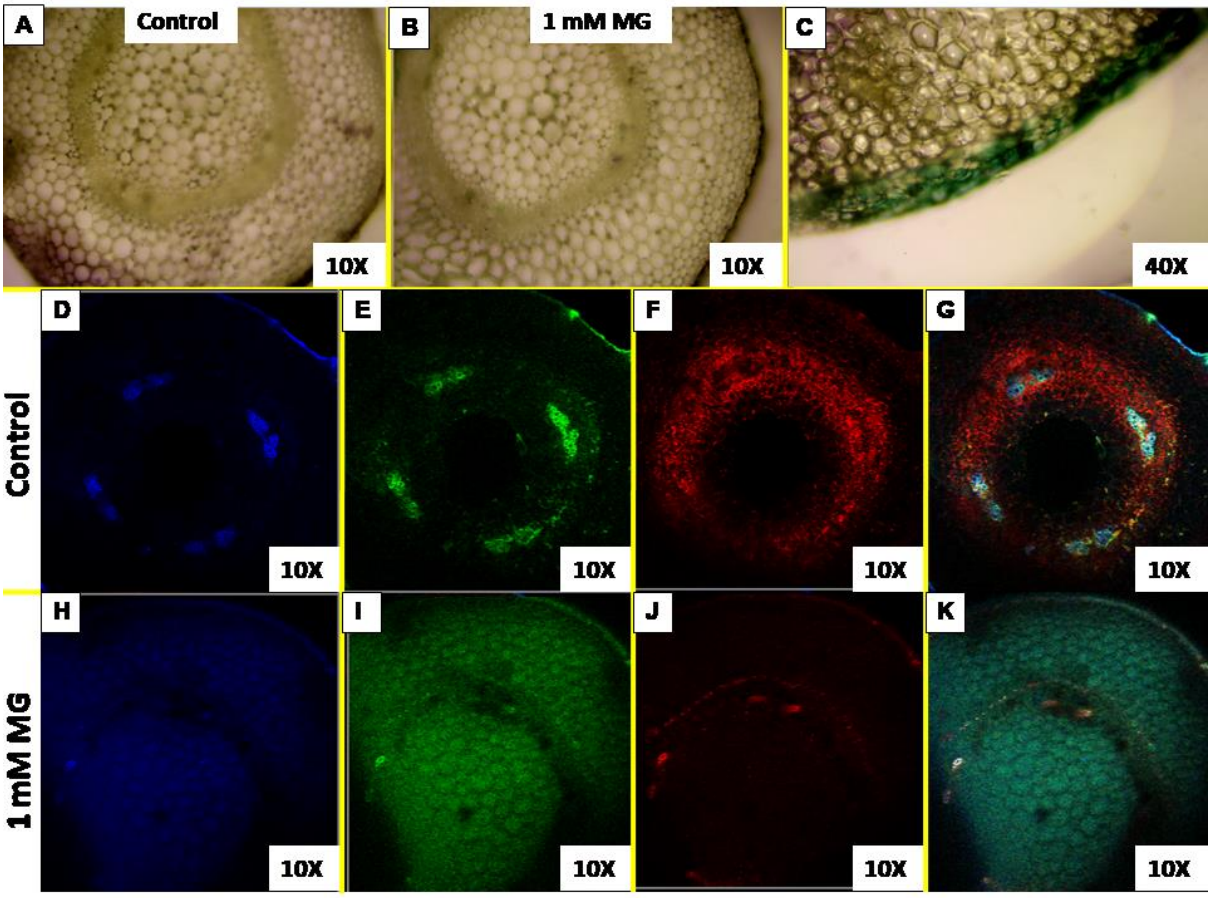

Figure 5.9: Bioimaging of mung bean (*Vigna radiata*) plant sections. (A) control root section (B) 1 mM exposed root section (C) Visible Adsorption of the dye by the epidermal layer (D-G) confocal images of control root section (H-K) confocal images of 1 mM exposed root section

5.2.7 Bioimaging of Mung Plant Sections

Transverse sections of mung plants (*Vigna radiata*) were cut with razor blades and studied for anatomical changes in the plant on exposure to MG (Figure 5.9). After 6 days of growth, the cross-sections of plant roots were viewed under optical light microscope for 1 mM MG and control sample plants (Figure 5.9A-B). No significant structural changes were observed in the morphology of the two sections. Figure 5.9C shows the adsorption of the dye by the epidermal layer and few outer parenchymal cells of the cortex after which subsequent imbibition through the vascular bundles gets either diminished or MG gets modified into an alternate form, like LMG, to get stored

in the cells. The roots of 1 mM MG and control mung samples were allowed to be immersed in CQD solution (0.33 mg/ml) for a few hours before confocal imaging of their transverse sections. The control plant images (Figure 5.9D-G) show brighter fluorescence near the vascular bundles particularly phloem and the outer epidermal tissue as reported earlier.[49,50] This shows the co-localization of the dye and CQDs in the epidermis, bound by weak interactions making ionic and hydrophobic bonds. CQDs have been postulated to cross the cell wall and plasmodesmata through apoplastic and symplastic pathways towards the cortex into the vascular system.[46] Plants grown in 0.4 mM also did not show a marked difference from the control and exhibited maximal fluorescence on the cortex parenchymal periphery and epidermis as seen earlier.[51] On the other hand, plants introduced to a high dose of MG (1 mM) exhibited significantly brighter fluorescence contributed by the CQDs as evident by brighter images for blue and green emission (Figure 5.9H-K). This may have been caused by the short length of the plants where more CQDs majorly get retained by the slowly differentiating tissues as opposed to the taller control plants which possessed a well-organized transport system and higher water content. Hence, CQDs can be used to differentiate between such tissues and can be explored further.

5.2.8 Effects of MG on animal cells (MG-63 cell line) and golden hamster

MG is a persistently used dye in various industries and has generated much attention due to its reported toxic effects. In a report describing human ingestion of this dye, symptoms of bronchitis and abdominal inflammation were observed.[13] Hyperventilation has often been reported in fish after MG consumption.[13] It has been reported to cause carcinogenesis, chromosomal damage, teratogenicity and respiratory toxicity in cell and animal models.[52-55] Further several reports have established that MG is a potent cytotoxic material for bacterial and mammalian cells.[55-58] MG can

cause decrease in food intake, growth and fertility rates and serious repercussions in lungs, bones and thyroid.[3] During festivals like Holi, it has been known to cause ocular epithelial defect.[14]

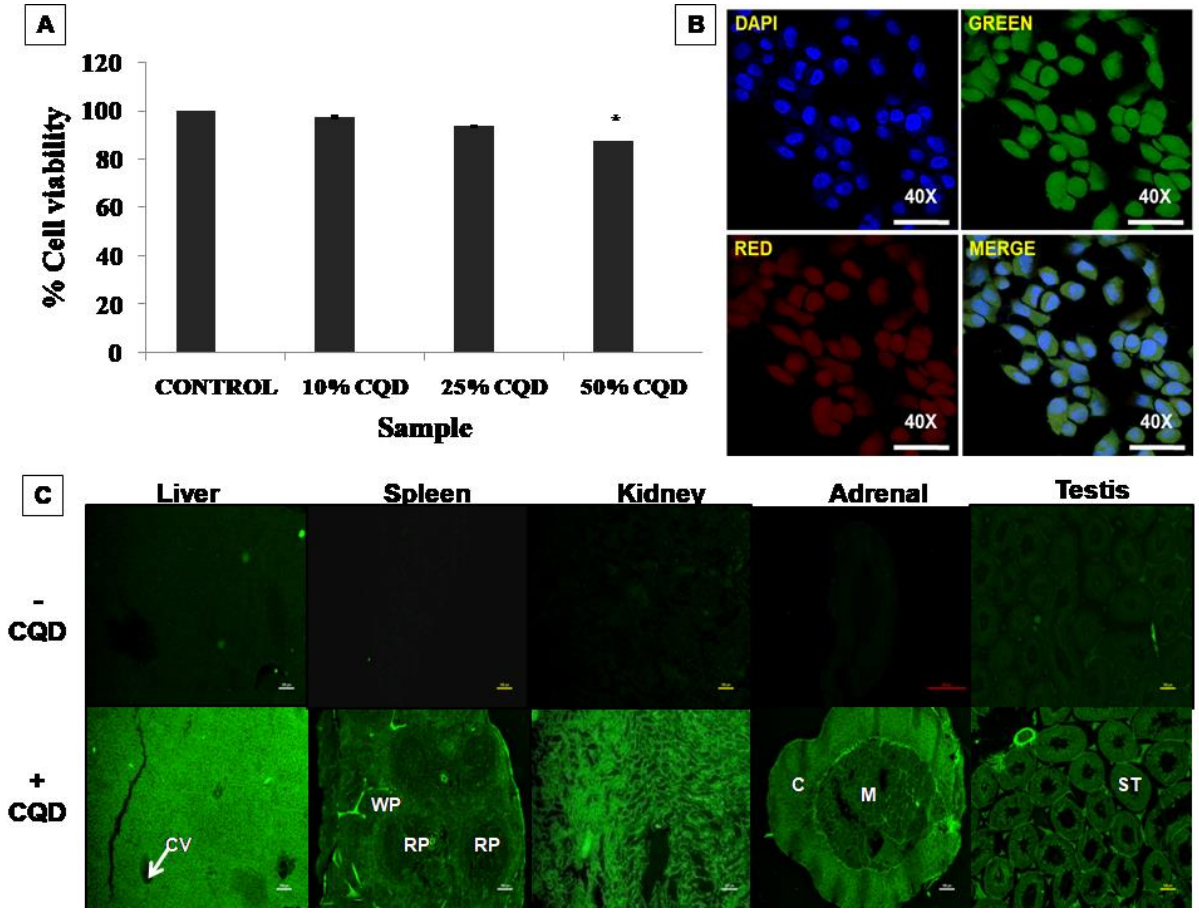

Figure 5.10: (A) Biocompatibility of CQDs in MG-63 cell line (B) Confocal imaging of cellular uptake analysis of CQD in MG-63 cells (C) Florescence imaging of organ tissues from animals administered CQD which reached the tissues via circulation

5.2.9 Biocompatibility of Sandalwood Derived CQDs at both cellular and tissue level

Luminescent carbon allotropes have received widespread research interests for biomedical applications due to their tunable optical properties and higher biocompatibility.[24] In this report, sandalwood-derived CQDs as bioimaging agents have been used. Dose-dependent MTT assay with 0.17 mg/ml or 50%, 0.08 mg/ml or 25% and 0.03 mg/ml or 10% CQD solution was performed in MG-63 cell line which

showed minimal cell death in comparison to control group (Figure 5.10A). Confocal microscopy confirmed cellular presence of CQD in both cytoplasm and nucleus (Figure 5.10B). These sandalwood-derived CQDs also showed wide spectral photoluminescence (blue-red). Decreased fluorescence intensity with decreased concentrations of CQD from the cells further supported the cell viability results (Figure 5.11).

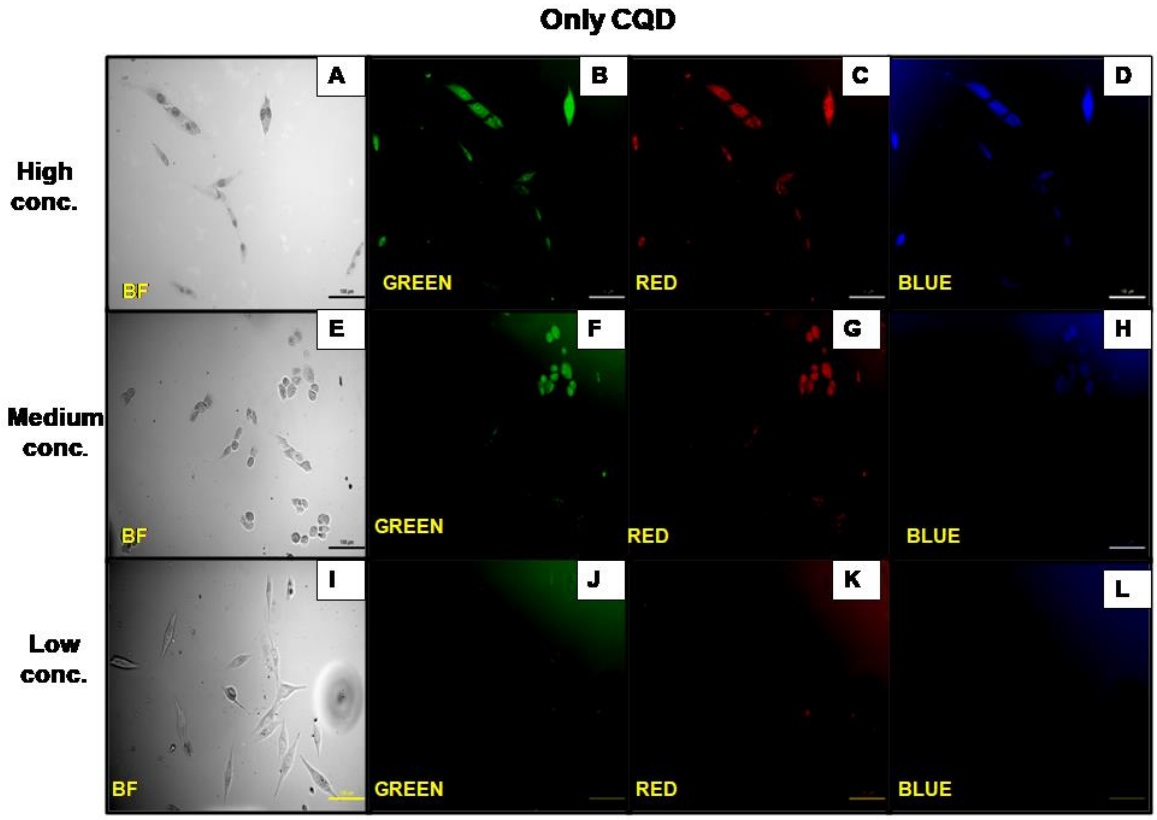

Figure 5.11: MG-63 cell proliferation in 3 doses of sandalwood-derived CQDs (0, 0.17, 0.33 µg/ml) clearly demonstrating fluorescence enhancement with increase in concentration

The organs of control animals exposed to CQDs only through internal intravenous injection were checked. The tissues showed bright luminescence conferred by CQDs in sections of liver, spleen, kidney, adrenal and testis after 24

hour treatment (Figure 5.10C). Thus 0.17 mg/ml or 50% concentration of CQD was selected for further bioimaging purpose.

5.2.10 CQD-Assisted Bioimaging for MG induced *in vitro* and *in vivo* morphometric changes

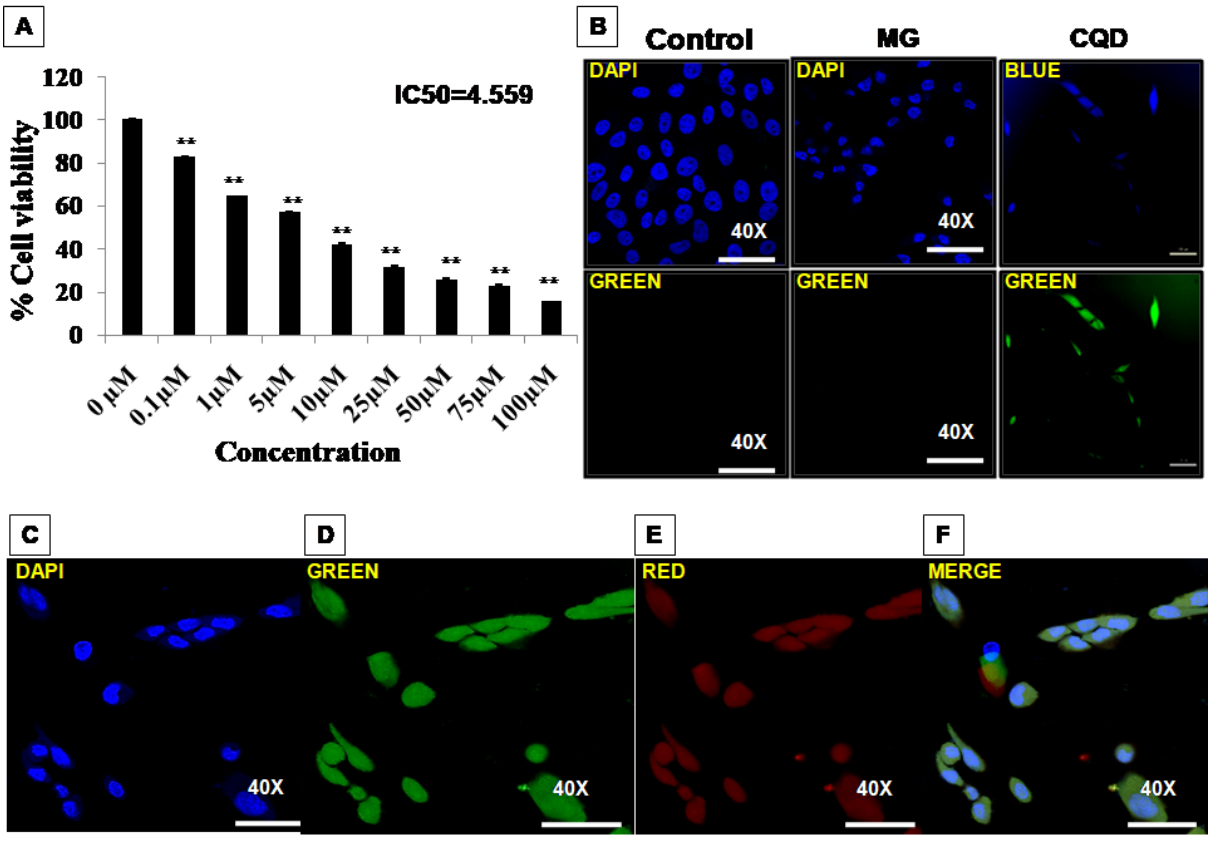

Figure 5.12: (A) Cell viability assay to analyse cellular toxicity caused by malachite green only (B) Confocal imaging of DAPI-stained control and MG-exposed MG-63 cells to prove MG causes nuclear blebbing in cells as compared to non-cytotoxic CQD-exposed cells (C) Confocal imaging of 4.5 uM MG exposed cells after DAPI+CQD staining showing apoptosis and cell distortion

In the present work, preliminary dose-dependent cell viability studies suggest dose-dependent decrease in cell viability of MG-63 cells. On increasing the concentration of MG, the calculated half maximal inhibitory concentration (IC50) was found to be 4.559 µM used for further experiments. This dose was further selected for

all biological studies (Figure 5.12A). The cellular toxicity of MG was further supported by DAPI staining studies on MG treated cells which induces morphological changes in cells with the formation of nuclear blebbing (Figure 5.12B). CQDs were observed to universally stain the MG-treated cells (Figure 5.12C-F). The blue emission of CQDs is shadowed by the higher fluorescence quantum yield of DAPI. These results suggest that CQDs may be used as effective bioimaging agents for future nuclear drug delivery applications. Previous reports also suggest that nuclei and mitochondria are the major cellular targets of MG while also proving damage to DNA.[5,6,59] This dye was reported to cause G2/M phase arrest in the cell cycle[2] along with high frequency of structural and numerical aberrations in somatic and germ cells.[5] It has also been seen that mitochondrial and nuclear cytotoxicity may be the result of generation of free radicals, lipid peroxidation and DNA adducts formation.[55]

Not only have the reports on *in vitro* studies confirmed the toxicity of MG, but also there were reports on rat and mice animal models which show the toxic effects of MG on various tissues especially liver and kidney.[2-8, 52] Therefore, dose dependent study on animal model i.e. male golden hamster was performed to find out the toxicological effects of MG in animals. The calculated half maximal lethal (LD50) dose was found to be 27 mg/kg body weight. Furthermore, previous chemical safety data has demonstrated acute oral LD50 of 50-120 mg/kg in mouse model.[6,7,13]

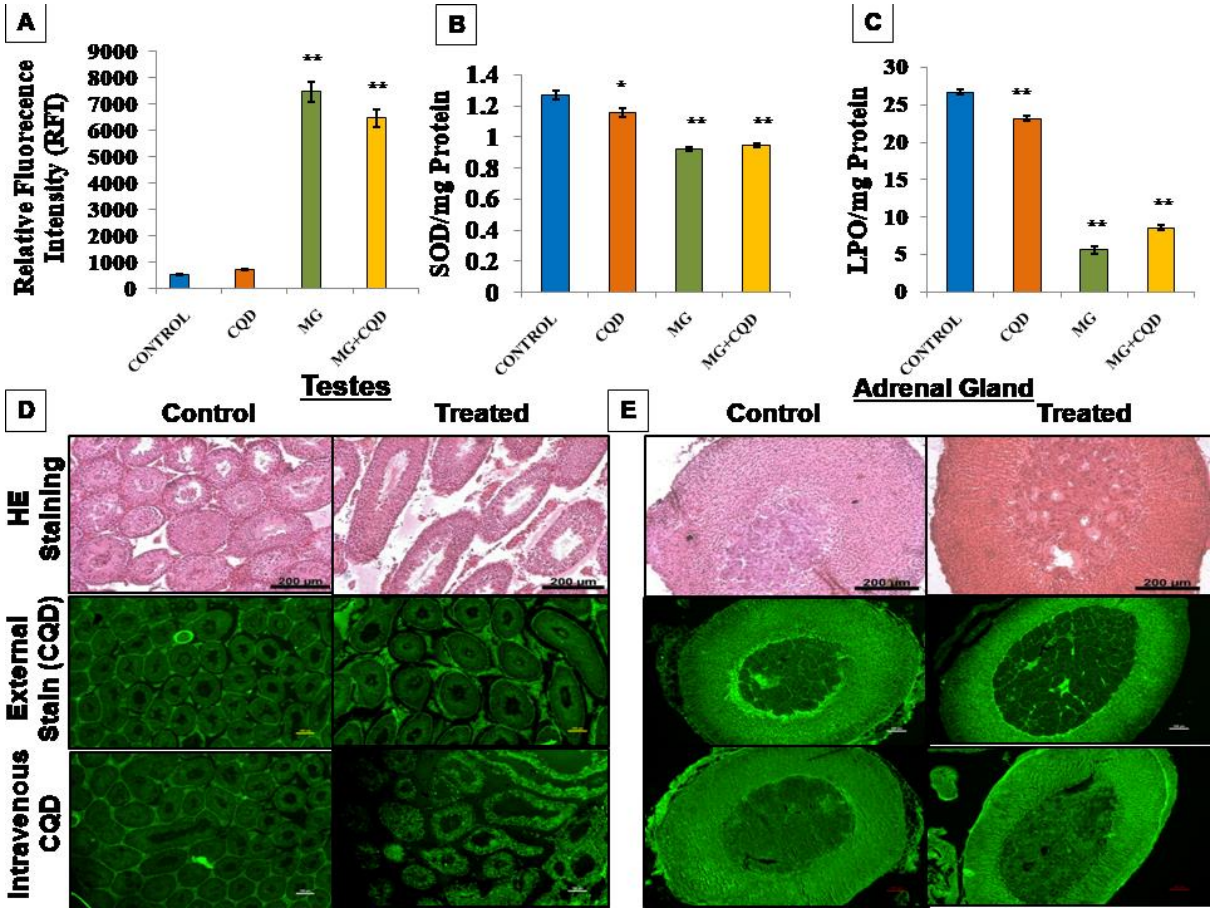

Figure 5.13: Biochemical analysis of ROS (A), SOD (B) and LPO (C) to show MG-induced free radical formation in animal serum. HE staining and CQD-Assisted fluorescence microscopic analysis to observe histological morphometric changes caused by MG in (D) testes (E) and adrenal gland tissues by externally applied and internally administered CQDs

To support MG toxicity, biochemical analysis of free radical load in the serum of golden hamsters was performed. The results suggest that MG increased free radical (Figure 5.13A) by significant decrease in SOD (Figure 5.13B) and lipid peroxidase enzyme concentrations (Figure 5.13C). This might be caused by MG-induced highly reactive metabolites in the chain of biochemical reactions. These results were further supported by previous reports on the overproduction of free radicals which may be associated with the depletion of glutathione S-transferases (GST) activity initiated by the presence of MG. Bcl2, p53, catalase activity and free radicals are reported to be

increased after malignant conversion.[5,9] Further reports in rats showed reduced motor activity, diarrhea, piloerection, hyperemia and atonia of the intestinal wall.[7] All together the results suggest MG is a potent environmental toxicant which may severely affect liver, adrenal gland, kidney and testes in golden hamsters. Toxicity level of CQDs was also measured in animal serum by ROS SOD, and LPO colorimetric analysis and no significant free radical generation was found after 24 hours intravenous exposure.

Control and MG-treated animals were autopsied and tissues from liver, kidney, adrenals, and testis were weighted and prepared for microscopy. On testes analysis, unhealthy small testes were found with tubular atrophy indicated by shrunken seminiferous tubules in MG-treated samples (Figure 5.13D). MG is known to have caused testicular changes and incomplete spermatogenisis in rats.[60] Human spermatozoa have been shown to be affected by the accumulation of MG at its plasma postacrosomal region.[38] Histopathological results and fluorescence imaging of adrenal tissue showed that larger adrenal medulla and smaller adrenal cortex diameter were observed in MG treated group as compared to the control group which may have been triggered by cellular stress (Figure 5.13E). Further bioimaging capability of CQDs was assessed *in vivo* in golden hamster model. CQDs have been used as a fluorophore both through intravenous delivery into circulation and as an external fluorescence stain in both control and MG treated animals. After 24 hours of CQDs application in golden hamster via intravenous injection, tissues showed bright luminescence conferred by CQDs in sections of liver, spleen, kidney, adrenal and testis. CQDs were further applied topically for bioimaging of MG-treated tissues to understand the morphological changes in adrenal and testes tissues through fluorescence imaging (Figure 5.13D-E). The superficial application of CQDs as a dye,

provided better resolution and structural detail of both control and MG-exposed groups as compared to standard staining protocols. Hence, CQDs might be use as alternative staining method. MG-treated liver and kidney HE sections clearly showed focal necrosis, atrophy and vacuolisation as described in many earlier reports (Figure 5.14).[3,16,61] Necrosis follows hypertrophy and vacuolisation. In liver, MG induces chromosomal aberrations and also affects the glucolytic-gluconeogenic pathway.[5]

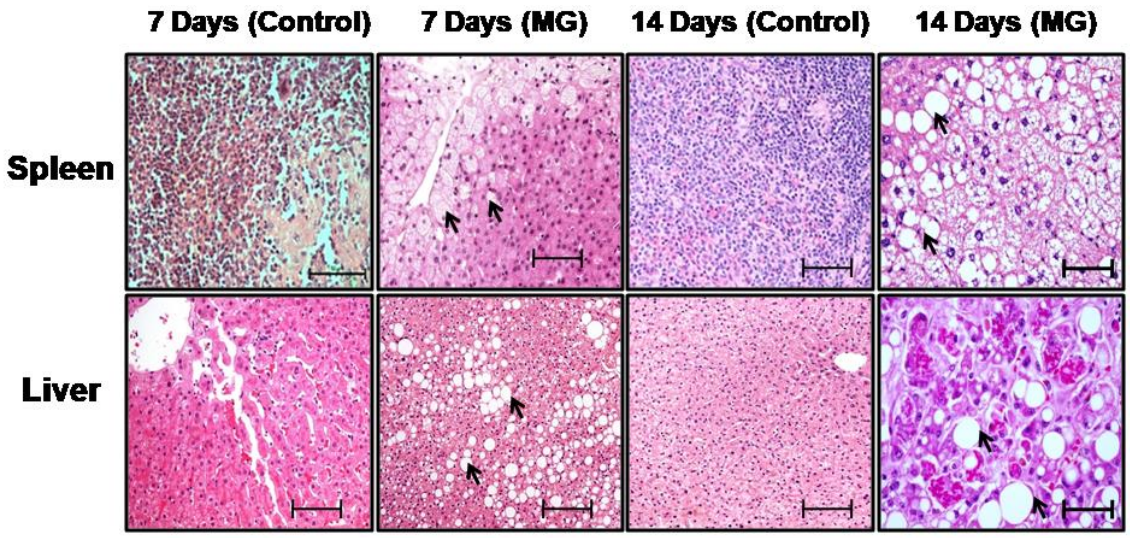

Figure 5.14: Morphological analysis of HE stained spleen and liver showing the histopathological changes between control and malachite green treated golden hamster after both 7 and 14 days of treatment. Arrows are showing the vacuolarization in both spleen and liver

This specific result opens the possibility for using CQDs as a fluorescent dye which could be used along with plant and animal cells and tissue staining method (HE staining) for better visualization and understanding of the tissue architectural changes. In summary we may conclude that sandalwood-derived CQDs can prove as excellent bioimaging tools having wide range of tissue acceptance via circulation or as an external stain which further could be used for future tissue specific biomedical studies.

5.3 Conclusions

To conclude, current study demonstrates the toxicological effects of a spuriously used common dye, malachite green in plant and animal cells and tissues. Our investigation shows that it affects both plant and animal physiologies and interferes with their proper growth and development. Onion tissues show the high affinity of MG for the nucleus and it linearly hampered the growth and development of mung plants (*Vigna radiata*). We successfully employed CQDs to differentiate between MG-exposed and control plant transverse section. Bioimaging of MG-63 cell line shows nuclear blebbing on exposure to MG. Dye exposure studies on golden hamster model in a dose-dependent manner helps in describing the toxicological effects on the testes and adrenal gland through bioimaging and suggests that future progeny may be adversely affected. Better visualisation and resolution of tissue architecture was enabled by CQD fluorescence imaging. In future, CQDs can be used as a general tissue and organ bioimaging tool to elucidate upon useful morphometric parameters that can help in building a stronger in-depth understanding of physiological changes.

5.4 References

[1] N. F. Robaina, L. G. T. dos Reis and R. J. Cassella. Diffuse reflectance determination of Malachite Green using polyurethane foam as solid support and sodium dodecylsulfate as counter ion. *Talanta* 85 (2011) 749–753.

[2] K. V. K. Rao, D. M. Mahudawala and A. A. Redkar. Malignant Transformation of Syrian Hamster Embryo (SHE) Cells in Primary Culture by Malachite Green: Transformation is Associated with Abrogation of G2/M Checkpoint Control. *Cell Biology International* 22 (1998) 581–589.

[3] S. Srivastava, R. Sinha and D. Roy. Toxicological effects of malachite green. *Aquatic Toxicology* 66 (2004) 319–329.

[4] S. J. Culp, P. W. Mellick, R. W. Trotter, K. J. Greenlees, R. L. Kodell and F. A. Beland. Carcinogenicity of malachite green chloride and leucomalachite green in B6C3F1 mice and F344 rats. *Food and Chemical Toxicology* 44 (2006) 1204–1212.

[5] S. M. Donya, A. A. Farghaly, M. A. Abo-Zeid, H. F. Aly, S. A. Ali, M. A. Hamed and N. S. El-Rigal. Malachite Green induces genotoxic effect and biochemical disturbances in mice. *European Review for Medical and Pharmacological Sciences* 16 (2012) 469-482.

[6] V. Fessard, T. Godard, S. Huet, A. Mourot and J. M. Poul. Mutagenicity of Malachite Green and Leucomalachite Green in *in vitro* Tests. *Journal of Applied Toxicology* 19 (1999) 421–430.

[7] S. Clemmensen, J. C. Jensen, N. J. Jensen, O. Meyer, P. Olsen and G. Wurtzen. Toxicological studies on malachite green: A triphenylmethane dye. *Archives of Toxicology* 56 (1984) 43-45.

[8] S. J. Culp, L. R. Blankenship, D. F. Kusewitt, D. R. Doerge, L. T. Mulligan and F. A. Beland. Toxicity and metabolism of malachite green and leucomalachite green during short-term feeding to Fischer 344 rats and B6C3F1 mice. *Chemico-Biological Interactions* 122 (1999) 153–170.

[9] D. M. Mahudawala, A. A. Redkar, A. Wagh, B. Gladstone and K. V. K. Rao. Malignant Transformation of Syrian Hamster Embryo (SHE) Cells in Culture by Malachite Green: An Agent of Environmental Importance. *Indian Journal of Experimental Biology* 37 (1999) 904-918.

[10] F. P. Meyer and T. A. Jorgenson. Teratological and Other Effects of Malachite Green on Development of Rainbow Trout and Rabbits. *Transactions of the American Fisheries Society* 112 (1983) 818-824.

[11] D. Shukla, F. P. Pandey, P. Kumari, N. Basu, M. K. Tiwari, J. Lahiri, R. N. Kharwar and A. S. Parmar. Label-Free Fluorometric Detection of Adulterant Malachite Green Using Carbon Dots Derived from the Medicinal Plant Source *Ocimum tenuiflorum*. *ChemistrySelect* 4 (2019) 4839–4847.

[12] K. Mitrowska, A. Posyniak and J. Zmudzki. The effects of cooking on residues of malachite green and leucomalachite green in carp muscles. *Analytica Chimica Acta* 586 (2007) 420–425.

[13] Md. Hisham, A. Vijayakumar, N. Rajesh and M. N. Sivakumar. Auramine-O and Malachite Green Poisoning: Rare and Fatal. *Indian Journal of Pharmacy Practice* 6 (2013) 72-74.

[14] T. Velpandian, K. Saha, A. K. Ravi, S. S. Kumari, N. R. Biswas and S. Ghose. Ocular hazards of the colors used during the festival-of-colors (Holi) in India—Malachite green toxicity. *Journal of Hazardous Materials* A139 (2007) 204–208.

[15] J. K. Das, S. Sarkar, Ugir H. Sk, P. Chakraborty, R. K. Das and S. Bhattacharya. Diphenylmethyl selenocyanate attenuates malachite green induced oxidative injury through antioxidation & inhibition of DNA damage in mice. *Indian Journal of Medical Research* 137 (2017) 1163-1173.

[16] M. Sundarrajan, S. Prabhudesai, S. C. Krishnamurthy and K. V. K. Rao. Effect of metanil yellow and malachite green on DNA synthesis in N-nitrosodiethylamine induced preneoplastic rat livers. *Indian Journal of Experimental Biology* 39 (2001) 845-852.

[17] J. R. Lawton. The use of malachite green during fixation of plant tissues for the preservation of lipids. *Journal of Microscopy* 144 (1986) 201-209.

[18] A. L. Henderson, T. C. Schmitt, T. M. Heinze and C. E. Cerniglia. Reduction of Malachite Green to Leucomalachite Green by Intestinal Bacteria. *Applied and Environmental Microbiology* 63 (1997) 4099–4101.

[19] S. Lee, J. Choi, L. Chen, B. Park, J. B. Kyong, G. H. Seong, J. Choo, Y. Lee, K. Shin, E. K. Lee, S. Joo and K. Lee. Fast and sensitive trace analysis of malachite green using a surface-enhanced Raman microfluidic sensor. *Analytica chimica acta* 590 (2007) 139-44.

[20] D. A. Navarro, M. A. Bisson, D. S. Aga. Investigating uptake of water-dispersible CdSe/ZnS quantum dot nanoparticles by *Arabidopsis thaliana* plants. *Journal of Hazardous Materials* 211–212 (2012) 427–435.

[21] P. Namdari, B. Negahdari, A. Eatemadi. Synthesis, properties and biomedical applications of carbon-based quantum dots: An updated review. *Biomedicine & Pharmacotherapy* 87 (2017) 209–222.

[22] Y. Wang and A. Hu. Carbon quantum dots: synthesis, properties and applications. *Journal of Materials Chemistry C* 2 (2014) 6921–6939.

[23] Z. Peng, X. Han, S. Li, A. O. Al-Youbi, A. S. Bashammakh, M. S. El-Shahawi, R. M. Leblanc. Carbon dots: Biomacromolecule interaction, bioimaging and nanomedicine. *Coordination Chemistry Reviews* 343 (2017) 256–277.

[24] J. Wang and J. Qiu. A review of carbon dots in biological applications. *Journal of Materials Science* 51 (2016) 4728–4738.

[25] A. N. A. Kumar, G. Joshi and H. Y. M. Ram. Sandalwood: history, uses, present status and the future. *Current Science* 103 (2012) 1-9.

[26] U. Subasinghe, M. Gamage, D.S. Hettiarachchi. Essential oil content and composition of Indian sandalwood (*Santalum album*) in Sri Lanka. *Journal of Forestry Research* 24 (2013) 127−130.

[27] M. J. Deka, P. Dutta, S. Sarma, O. K. Medhi, N. C. Talukdar, D. Chowdhury. Carbon Dots derived from water hyacinth and their application as a sensor for pretilachlor. *Heliyon* 5 (2019)

[28] X. Gong, W. Lu, M. C. Paau, Q. Hu, X. Wu, S. Shuang, C. Dong, M. M. F. Choi. Facile synthesis of nitrogen-doped carbon dots for Fe^{3+} sensing and cellular imaging. *Analytica Chimica Acta* 861 (2015) 74-84

[29] V. Ramanan, T. S. Kumar, R. Kaviyarasan, R. Suresh, S. Rajkumar, P. Ramamurthy. An Outright Green Synthesis of Fluorescent Carbon Dots from Eutrophic Algal Blooms for *In Vitro* Imaging. *ACS Sustainable Chemical Engineering* 4 (2016) 4724-4731.

[30] V. N. Mehta, S. Jha, H. Basu, R. K. Singhal, S. K. Kailasa. One-step hydrothermal approach to fabricate carbon dots from apple juice for imaging of mycobacterium and fungal cells. *Sensors and Actuators B* 213 (2015) 434–443.

[31] C. X. Guo, J. Xie, B. Wang, X. Zheng, H. B. Yang and C. M. Li. A new class of fluorescent-dots: long luminescent lifetime bio-dots self-assembled from DNA at low temperatures. *Scientific Reports* 3 (2013) 2957 1-6.

[32] S. Kalytchuk, Y. Wang, K. Polaˇkova´, R. Zbor´ il. Carbon Dot Fluorescence-Lifetime-Encoded Anti-Counterfeiting. *ACS Appl. Mater. Interfaces* 10 (2018) 29902−29908.

[33] M. Y. Berezin, S. Achilefu. Fluorescence Lifetime Measurements and Biological Imaging. *Chem. Rev.* 110 (2010) 2641–2684.

[34] S. Mitra, S. Chandra, T. Kundu, R. Banerjee, P. Pramanik and A. Goswami. Rapid microwave synthesis of fluorescent hydrophobic carbon dots. *RSC Advances* 2 (2012) 12129–12131.

[35] S. Timofei, L. Kurunczi, W. Schmidt and Z. Simon. Lipophilicity in Dye-Cellulose Fibre Binding. *Dyes and Pigments* 32 (1996) 2542.

[36] F. Jiang, D. M. Dinh, Y. Hsieh. Adsorption and desorption of cationic malachite green dye on cellulose nanofibril aerogels. *Carbohydrate Polymers* 173 (2017) 286–294.

[37] Z. Aihua, G. Qiang, H. Quanguo, G. Rong and Y. Chunwei. Interaction of malachite green with lecithin liposomes. *Colloids and Surfaces A: Physicochemical Engineering Aspects* 224 (2003) 75-82.

[38] P. Soupart, M. L. Anderson, D. H. Albert, J. G. Coniglio, J. E. Repp. Accumulation, Nature and Possible Functions of the Malachite Green Affinity Material in Ejaculated Human Spermatozoa. Fertility and Sterility 32 (1979) 450-454.

[39] C. Yu, T. Xuan, D. Yan, S. Lou, X. Hou, Y. Chen, J. Wang and H. Li. Sesame-derived ions co-doped fluorescent carbon nanoparticles for bio-imaging, sensing and patterning applications. *Sensors and Actuators B* 253 (2017) 900–910.

[40] W. Li, Y. Zheng, H. Zhang, Z. Liu, W. Su, S. Chen, Y. Liu, J. Zhuang and B. Lei. Phytotoxicity, Uptake, and Translocation of Fluorescent Carbon Dots in Mung Bean Plants. *ACS Applied Materials Interfaces* 8 (2016) 19939 −19945.

[41] H. Wang, M. Zhang, Y. Song, H. Li, H. Huang, M. Shao, Y. Liu and Z. Kang. Carbon dots promote the growth and photosynthesis of mung bean sprouts. *Carbon* 136 (2018) 94-102.

[42] M. Monici. Cell and tissue autofluorescence research and diagnostic applications. *Biotechnology Annual Review* 11 (2005) 227-256.

[43] H. P. Singh, D. R. Batish, R. K. Kohli and K. Arora Arsenic-induced root growth inhibition in mung bean (*Phaseolus aureus Roxb.*) is due to oxidative stress resulting from enhanced lipid peroxidation. *Plant Growth Regulators* 53 (2007) 65–73.

[44] J. P. Jadhav and S. P. Govindwar. Biotransformation of malachite green by *Saccharomyces cerevisiae* MTCC 463. *Yeast* 23 (2006) 315–323.

[45] R. Gopinathan, J. Kanhere and J. Banerjee. Effect of malachite green toxicity on non target soil organisms. *Chemosphere* 120 (2015) 637–644.

[46] S. Tripathi and S. Sarkar. Influence of water soluble carbon dots on the growth of wheat

plant. *Applied Nanoscience* (2015) 5:609–616.

[47] S. Chandra, S. Pradhan, S. Mitra, P. Patra, A. Bhattacharya, P. Pramanik and A. Goswami. High throughput electron transfer from carbon dots to chloroplast: A rationale of enhanced photosynthesis. *Nanoscale* 6 (2014) 3647-3655.

[48] P. Matpang, M. Sriuttha, N. Piwpuan. Effects of malachite green on growth and tissue accumulation in pakchoy (*Brassica chinensis* Tsen & Lee). *Agriculture and Natural Resources* 51 (2017) 96-102.

[49] Y. Li, J. Bi, S. Liu, H. Wang, C. Yu, D. Li, B. Zhu and M. Tan. Presence and Formation of Fluorescence Carbon Dots in Grilled Hamburger. *Food Function* 8 (2017) 2558–2565.

[50] M. Zhang, L. Hu, H. Wang, Y. Song, Y. Liu, H. Li, M. Shao, H. Huang and Z. Kang. One-step hydrothermal synthesis of chiral carbon dots and their effects on mung bean plant growth. *Nanoscale* 10 (2018) 12734–12742.

[51] B. Lin, Y. Yu, F. Liu, Y. Cao and M. Guo. Tunable and Nontoxic Fluorescent Probes Based on Carbon Dots for Imaging of Indole Propionic Acid Receptor in Plant Tissues *in situ*. *Journal of Fluorescence* 27 (2017) 1495–1503.

[52] K. V. K. Rao. Inhibition of DNA synthesis in primary rat hepatocyte cultures by malachite green: a new liver tumor promoter. Toxicology Letters 81 (1995) 107-113.

[53] C. Fernandes, V. S. Lalitha, V. K. Rao. Enhancing eVects of malachite green on the development of hepatic preneoplastic lesions induced by N-nitroso diethylamine in rats. *Carcinogenesis* 12 (1991) 839–845.

[54] S. Srivastava, R. Sinha, D. Roy. Toxicological eVects of malachite green. Aquatic Toxicology 66 (2004) 319–329.

[55] A. Stammati, C. Nebbia, I. D. Angelis, A. G. Albo, M. Carletti, C. Rebecchi, F. Zampaglioni, M. Dacasto. Effects of malachite green (MG) and its major metabolite, leucomalachite green (LMG), in two human cell lines. *Toxicology in Vitro* 19 (2005) 853–858.

[56] E. Sudova, J. Machova, Z. Svobodova, T. Vesely. Negative effects of malachite green and possibilities of its replacement in the treatment of fish eggs and fish: A review. *Veterinarni Medicina* 52 (2007) 527–539.

[57] H. H. Pfeiffer. Malachitgrun Effekt em dritten Autosom der Speicheldrusenk-erne von Drosophila-Larven. Exp Cell Res 22 (1961) 356-362.

[58] D. J. Alderman and R. S. Clifton-Hadley. Malachite Green: A Pharmakokinetic Study in Rainbow Trout, Oncorhynchus mykiss (Walbaum). *Journal of Fish Diseases* 16 (1993) 297-311.

[59] B. Bose, L. Motiwale and K.V.K. Rao. DNA damage and G2/M arrest in Syrian hamster embryo cells during Malachite green exposure are associated with elevated phosphorylation of ERK1 and JNK1. *Cancer Letters* 230 (2005) 260–270.

[60] M. G. Allmark, H. C. Grice and W. A. Mannell. Chronic Toxicity Studies on Food Colours. *Journal of Pharmacy and Pharmacology* 8 (1956) 417-24.

[61] A. Stammati, C. Nebbia, I. de Angelis, A. G. Albo, M. Carletti, C. Rebecchi, F. Zampaglioni and M. Dacasto. EVects of malachite green (MG) and its major metabolite, leucomalachite green (LMG), in two human cell lines.